www.lajss.org
Latin American Journal of Solids and Structures 2 (2005) 153–165

A nonlocal model for size effect and localization in plasticity

C. Comi[a,*] and L. Driemeier[b]

[a]Dept. Structural Engineering, Politecnico di Milano, Piazza L. da Vinci 32 - 20133 Milano
[b]Dept. Mechatronics and Mechanical Systems Engineering, University of Sao Paulo, Av. Prof. Mello Moraes, 2231, 05508-900, Sao Paulo, Brazil

Abstract

A simple nonlocal plasticity model is proposed to account for the size dependence of plastic deformation at the micro-scale and at the same time to regularize the response in the presence of localization phenomena. Nonlocality is introduced in the yield function through the definition of a nonlocal strain, which is the weighted average of the local strain over a suitable neighborhood, depending on the material length. We apply the model to a strain localization problem of a softening bar and we compare model predictions with experiments on microbending and microtorsion.

1 Introduction

Classical local plasticity theory, in which no length scale enters, disregards the influence of the microscopic material structure on the macroscopic material behaviour. Although local theories are able to interpret the material behavior in a large number of applications, they become inadequate to model phenomena such as the experimentally observed size-dependence of the plastic response of micro-sized solids or the appearance of localization bands of finite width in the presence of softening or very large strains.

In particular, tests performed at the micro- or nano-scale such as nano-indentation [3, 27, 28, 32], bending of thin metallic beams [21, 31] or micro-torsion of thin copper wires [17] have provided experimental evidence of strain gradient hardening, which makes the response dependent on the scale of the structure. Hardness and strength increase as the specimen size is decreased; this size effect, which is negligible for macro-specimen, becomes important at very small scales and cannot be captured by local models.

Another noteworthy example is the localization phenomenon. Strain localization is characterized by pronounced displacement gradients – induced by geometry, boundary conditions, material heterogeneity or local defects – in restrict zones of the medium, called strain localization zones. With local models, the width of the localization zones tend to zero, with the nowadays well known numerical consequences in terms of pathological mesh dependence. As

*Corresponding author Email: comi@stru.polimi.it Received 15 June 2005; In revised form 22 June 2005

pointed out in [7, 24], mathematically, the boundary value problem becomes ill-posed and the model no longer represents the physical reality.

The ill-posedness of the problem can be overcame by using regularization techniques, providing accurate numerical solutions. Nonlocal gradient models [8,10,13], nonlocal integral models [5, 9, 29] and micropolar models [30] which include a material internal length have been formulated and effectively used.

Enhanced gradient models have also been used to interpret size effect at the microscale, see [1,2,4,16,18,20,23,25]. These models allow to account for the presence of geometrically necessary dislocations whose accumulation increases the flow stress; this effect becomes important when the scale of the specimen approaches the scale of the lattice. Gradient plasticity formulations lead to the definition of one or more internal length parameters, or even internal length tensors, whose values can be identified on the basis of sophisticated tests and/or atomistic considerations [15,17]. Gao and Huang in [19] explore the possibility of modeling size-dependent plasticity within the framework of nonlocal continuum theories. Considering the Taylor expansion of the strain, they represent strain gradient as a nonlocal integral of strain

In this work we propose an alternative nonlocal plastic model intended to capture the material behavior at the microscale and at the same time to regularize the response in the presence of localization phenomena. Nonlocality is introduced in the yield function through the definition of a nonlocal strain which is the weighted average of the local strain over a suitable neighborhood depending on the material length. Similarly to the so-called *lower order strain gradient plasticity theory* [4, 26], this formulation does not require any additional stress quantity or boundary condition.

The effectiveness of the proposed model to reproduce size effect at the micro-scale is checked by simulating the experimental results concerning microbending of thin films and micro-torsion of thin wires. The regularization properties of the nonlocal formulation are evidenced with reference to the simple one-dimensional problem of tension in a softening bar.

2 Formulation

We consider the elastoplastic evolution of a body Ω. The constitutive model is expressed by the following state equations, loading-unloading conditions and evolutive equations

$$\boldsymbol{\sigma} = \boldsymbol{E} : (\varepsilon - \varepsilon^p), \qquad \boldsymbol{\chi} = \boldsymbol{\chi}(\boldsymbol{\eta}) \tag{1}$$

$$f(\boldsymbol{\sigma}, \boldsymbol{\chi}) \leq 0, \qquad \dot{\lambda} \geq 0, \qquad f\dot{\lambda} = 0 \tag{2}$$

$$\dot{\varepsilon}^p = \frac{\partial g(\boldsymbol{\sigma}, \boldsymbol{\chi})}{\partial \boldsymbol{\sigma}} \dot{\lambda}, \qquad \dot{\boldsymbol{\eta}} = -\frac{\partial g(\boldsymbol{\sigma}, \boldsymbol{\chi})}{\partial \boldsymbol{\chi}} \dot{\lambda} \tag{3}$$

where $\boldsymbol{\sigma}$ is the stress tensor, ε and ε^p are the total and plastic strain tensors, $\boldsymbol{E}$ is the elasticity tensor, $\boldsymbol{\eta}$ is a set of internal variables describing hardening, $\boldsymbol{\chi}$ are the thermodynamic forces

conjugate to $\boldsymbol{\eta}$, f is the yield function, $\dot{\lambda}$ is the plastic multiplier and g the inelastic potential. A generalization of the above local plasticity model is here proposed to account for size effect at the microscale and to deal with localization problems. An internal material length ℓ is introduced in the model in order to account for nonlocal interactions in the inelastic behaviour. A nonlocal yield function $\bar{f}$ is defined which depends on an integral nonlocal total strain measure $\bar{\boldsymbol{\varepsilon}}(\boldsymbol{x})$

$$\bar{\boldsymbol{\varepsilon}}(\boldsymbol{x}) = \int_{\Omega} W(\boldsymbol{x}-\boldsymbol{\xi})\,\boldsymbol{\varepsilon}(\boldsymbol{\xi})\,\mathrm{d}\boldsymbol{\xi} \tag{4}$$

$W(\boldsymbol{x}-\boldsymbol{\xi})$ being a weight function. A possible choice for W is the Gaussian weight function, as proposed in [9, 29],

$$W(\boldsymbol{x}-\boldsymbol{\xi}) = \frac{1}{W_0(\boldsymbol{x})}\exp\left(\frac{-\|\boldsymbol{x}-\boldsymbol{\xi}\|^2}{2\ell^2}\right) \quad \text{with} \quad W_0(\boldsymbol{x}) = \int_{\Omega}\exp\left(\frac{-\|\boldsymbol{x}-\boldsymbol{\xi}\|^2}{2\ell^2}\right)\mathrm{d}\boldsymbol{\xi} \tag{5}$$

The parameter ℓ represents an internal scale, which is considered a material parameter with dimension of a length. This parameter defines the dimension of the neighborhood that affects the non-local function. Note that the average is extended to the whole volume Ω, but due to the shape of the weigth function, the material parameter ℓ defines the region of the body, surrounding point $\mathbf{x}$, which really influences the behaviour at that point. The nonlocal strain tensor $\bar{\boldsymbol{\varepsilon}}$ is only used in the yield function, while state equations remain in the local form (1). In the following, for simplicity, we will restrict to isotropic hardening/softening case described by a single scalar internal variable η; in this case the nonlocal yield function can be written as

$$\bar{f}(\boldsymbol{\sigma},\chi) = \varphi(\boldsymbol{E} : (\bar{\boldsymbol{\varepsilon}} - \boldsymbol{\varepsilon}^p)) - \chi(\eta) \tag{6}$$

where φ is an equivalent stress (e.g. Mises or Drucker-Prager equivalent stress).

The linear strain-displacement relation and equilibrium equations are the conventional one

$$\boldsymbol{\varepsilon} = \frac{1}{2}\left(grad^T\,\boldsymbol{u} + grad\boldsymbol{u}\right) \tag{7}$$

$$div\boldsymbol{\sigma} = \boldsymbol{F} \qquad \boldsymbol{\sigma}^T = \boldsymbol{\sigma} \tag{8}$$

where $\boldsymbol{F}$ is the body force vector.

The nonlocal boundary value problem above defined is always elliptic, also in the presence of softening behaviour, as proved in [11]. A bifurcation analysis shows that the characteristic length ℓ of the model fixes the wavelength of possible bifurcated solutions, thus preventing strain localization into a line of zero thickness.

2.1 Mises flow theory

Let us decompose total and plastic strains and stresses into their deviatoric ($\boldsymbol{e}, \boldsymbol{e}^p$, $\boldsymbol{s}$) and volumetric parts ($tr\boldsymbol{\varepsilon}$,$tr\boldsymbol{\varepsilon}^p$,$tr\boldsymbol{\sigma}$)

$$\boldsymbol{\varepsilon} = \boldsymbol{e} + \frac{tr\boldsymbol{\varepsilon}}{3}\mathbf{1}, \qquad \boldsymbol{\varepsilon}^p = \boldsymbol{e}^p + \frac{tr\boldsymbol{\varepsilon}^p}{3}\mathbf{1}, \qquad \boldsymbol{\sigma} = \boldsymbol{s} + \frac{tr\boldsymbol{\sigma}}{3}\mathbf{1} \tag{9}$$

According to Mises plasticity, the volumetric behaviour is assumed to be purely elastic, thus the state equations can be written as

$$tr\,\boldsymbol{\sigma} = 3Ktr\boldsymbol{\varepsilon}, \qquad \boldsymbol{s} = 2G\left(\boldsymbol{e} - \boldsymbol{e}^p\right) \tag{10}$$

K and G being the bulk and shear modulus, respectively.

The yield condition for the non local mises flow theory reads

$$\bar{f}\left(\boldsymbol{\sigma},\chi\right) = \bar{\sigma}_{eq} - \chi\left(\eta\right) = 2\mu\sqrt{\frac{3}{2}\left(\bar{\boldsymbol{e}} - \boldsymbol{e}^p\right) : \left(\bar{\boldsymbol{e}} - \boldsymbol{e}^p\right)} - \chi\left(\eta\right) \tag{11}$$

where $\bar{\boldsymbol{e}}$ is the nonlocal deviatoric strain. Plastic strain rates and internal variables rates are given by normality rules

$$\dot{\boldsymbol{e}}^p = \frac{3\boldsymbol{s}}{\bar{\sigma}_{eq}}\dot{\lambda}, \qquad \dot{\eta} = \dot{\lambda} \tag{12}$$

where $\dot{\lambda}$ is the plastic multiplier to be determined by the loading-unloading conditions (2).

2.2 Deformation theory

The deformation theory for the proposed model assumes the same structure of classical deformation theory [22]. The total deviatoric strain are assumed proportional to deviatoric stresses

$$\boldsymbol{e} = \alpha\boldsymbol{s} \tag{13}$$

The nonlocal yield function thus becomes

$$\bar{f}\left(\boldsymbol{\sigma},\chi\right) = \bar{\sigma}_{eq} - \chi\left(\eta\right) = \frac{\sqrt{\frac{3}{2}\bar{\boldsymbol{e}} : \bar{\boldsymbol{e}}}}{\alpha} - \chi\left(\eta\right) \tag{14}$$

Under full loading assumption the coefficient α is given by

$$\alpha = \frac{\sqrt{\frac{3}{2}\bar{\boldsymbol{e}} : \bar{\boldsymbol{e}}}}{\chi\left(\eta\right)} \tag{15}$$

The volumetric behaviour is linear elastic as in the flow theory.

3 Applications

3.1 Tension of a softening bar

We consider an elastoplastic softening bar subject to an imposed axial displacement u. This classical example has been extensively explored in the literature to demonstrate the shortcomings of a local model and the efficiency of proposed regularization techniques, see e.g. [6, 8, 14]. For

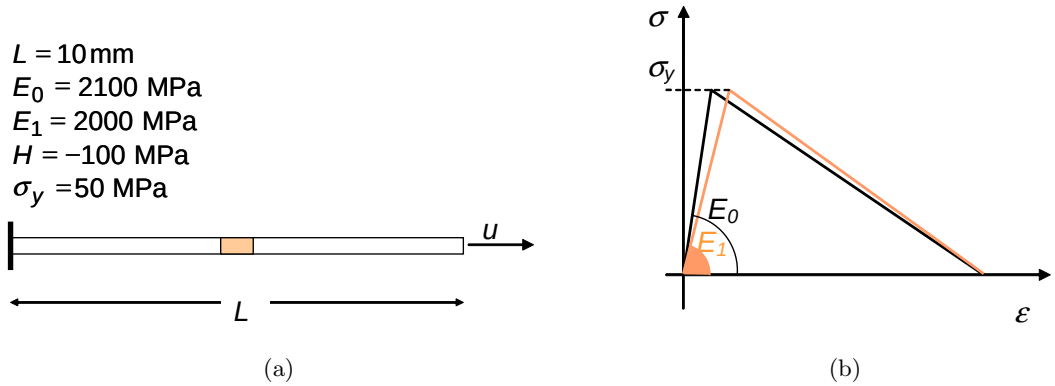

(a) (b)

Figure 1: Uniaxial tension test: (a) geometry and material data (b) linear softening law

this one dimensional example only one stress component σ is considered and, assuming linear softening behaviour, the flow theory of the nonlocal model can be expressed as

$$\bar{f}(\sigma,\chi) = E(\bar{\varepsilon} - \varepsilon^p) - \chi(\eta), \quad \chi = \sigma_y + H\eta, \quad \dot{\varepsilon}^p = \dot{\eta} = \dot{\lambda} \tag{16}$$

with $\bar{\varepsilon}$ defined as in eq.(4). E is the Young modulus, σ_y is the initial yield limit and $H < 0$ is the softening parameter (see Figure 1). The central part of the bar is weakened (5 % reduction of the Young's modulus) to trigger localization; E_1 and E_o are respectively the Young's moduli in the weakened central part and in the rest of the bar. Numerical analyses, both with the local and nonlocal formulations (with material internal length $\ell = 0.19$mm) have been carried out using three different meshes of constant strain bar elements. The nonlocal procedure has required to modify the predictor-correction iterative solution scheme, adding an averaging phase between predictor and corrector to compute the nonlocal strain $\bar{\varepsilon}$. An arc-length procedure has been used to follow possible snap- back behaviour.

Figure 2 shows the numerical response in terms of reaction versus imposed displacement obtained with the different meshes. The response obtained with the local model, figure 2a exhibit pathological mesh dependence: as the mesh is refined the numerical response becomes more brittle and tends to the unphysical prediction of failure with zero dissipation. The results obtained with the proposed nonlocal model are shown in figure 2b. Convergence to a physically acceptable solution with a well-defined positive dissipation is observed. The plastic strain profile for $u = 0.6$ mm, figure 3, is also almost mesh-independent and evidences a localization zone depending on the material internal length ℓ and not on the element size.

3.2 Bending of thin beams

The nonlocal model here proposed is used to simulate the microbend tests reported in [31] which give evidence of the size effect at the micron scale. Bending of ultra-thin beams is considered

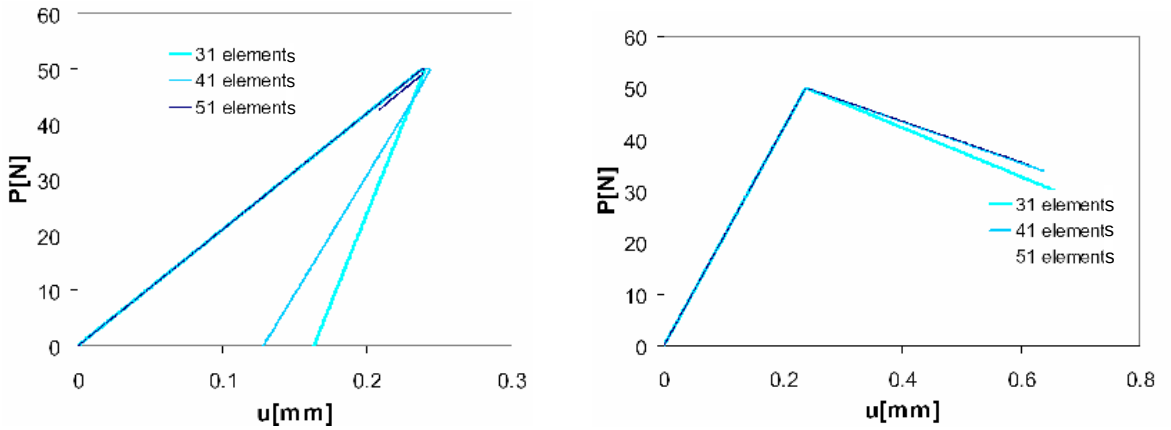

(a) (b)

Figure 2: Reaction vs displacement curves for different meshes (a) local model; (b) nonlocal model.

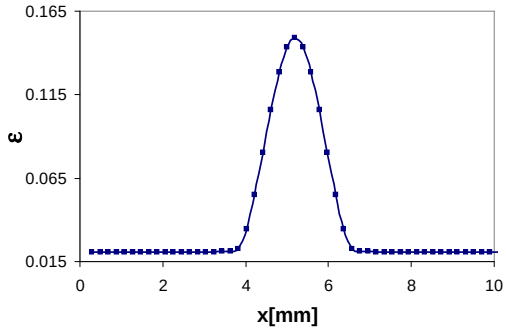

Figure 3: Plastic deformations along the bar, nonlocal model

under plane strain conditions. The reference frame is defined in figure 4, bending is applied in the $x_1 - x_2$ plane.

Since bending moment is monotonically increased, the deformation theory is used in this example and, for simplicity, elastic deformation is neglected. With the above hypotheses, the beam theory gives:

$$\varepsilon_{11} = e_{11} = \kappa x_2; \quad \varepsilon_{22} = e_{22} = -\kappa x_2; \quad \varepsilon_{33} = \varepsilon_{12} = \varepsilon_{13} = \varepsilon_{23} = 0 \tag{17}$$

where κ is the curvature. The nonvanishing nonlocal strain components are

$$\bar{\varepsilon}_{11} = -\bar{\varepsilon}_{22} = \frac{\int_{-\frac{h}{2}}^{\frac{h}{2}} \exp\left(\frac{-\|x_2-\xi\|^2}{2\ell^2}\right) \kappa\xi d\xi}{\int_{-\frac{h}{2}}^{\frac{h}{2}} \exp\left(\frac{-\|x_2-\xi\|^2}{2\ell^2}\right) d\xi} \tag{18}$$

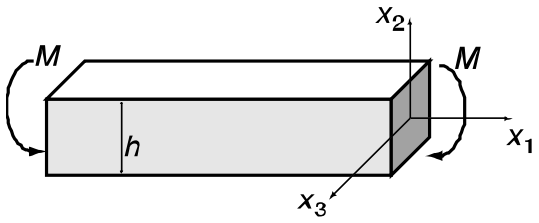

Figure 4: Microbending: geometry

Figure 5 shows the variation of $\bar{\varepsilon}_{11}$ along the beam thickness (axes are normalized), for different values of the ratio $\frac{\ell}{h}$ between internal material length and the beam height. As $\ell \to 0$ or h$\to \infty$, the local linear distribution is approached; for a given material (ℓ fixed) the nonlocal effect becomes important for small scale specimen.

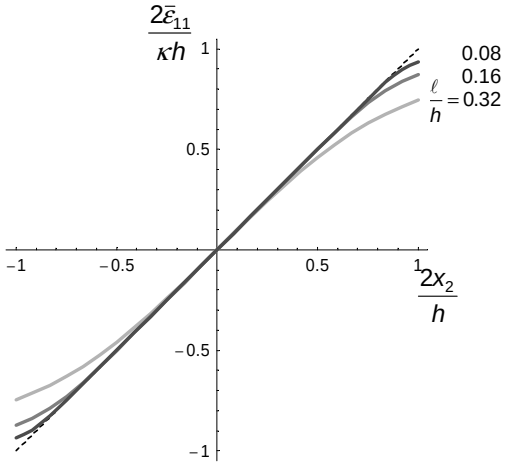

Figure 5: Nonlocal strain

In the deformation theory deviatoric stresses are proportional to deviatoric strains through eq. (13), therefore, due to (17), one has

$$s_{11} = -s_{22} \tag{19}$$

The equilibrium in the bulk and the traction free boundary conditions al $x_2 = \pm\frac{h}{2}$ entail

$$\sigma_{22} = 0 \tag{20}$$

and, hence, give the hydrostatic stress and the normal stress to the cross section

$$tr\boldsymbol{\sigma} = -3s_{22}, \quad \sigma_{11} = 2s_{11} \tag{21}$$

The bending moment can be finally computed as

$$M = \int_{-\frac{h}{2}}^{\frac{h}{2}} 2 s_{11} x_2 dx_2 = \int_{-\frac{h}{2}}^{\frac{h}{2}} 2 \frac{\chi}{\sqrt{\frac{3}{2}\left(\bar{\varepsilon}_{11}^2 + \bar{\varepsilon}_{22}^2\right)}} \kappa x_2 x_2 dx_2 \tag{22}$$

Linear isotropic hardening $\chi = \sigma_0 + H\varepsilon$, with parameters σ_0 and H taken from the microtensile tests of [31], has been assumed for the simulation. Figure 6 compares the experimental results of [31] with the prediction of the proposed model (with $\ell = 4\ \mu m$) in terms of non-dimensional bending moment ($\frac{4M}{\sigma_0 b h^2}$) versus maximum strain $\kappa\frac{h}{2}$: good agreement is found.

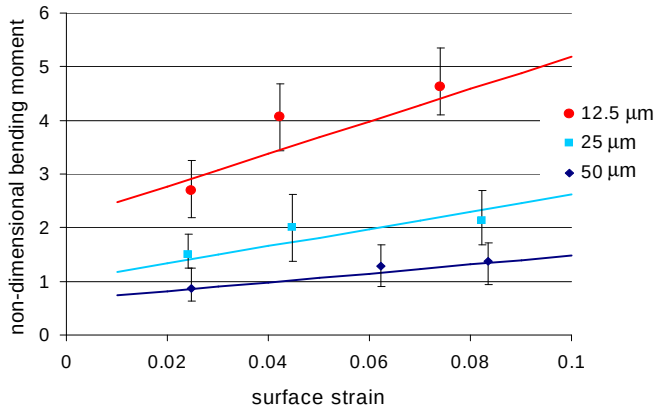

Figure 6: Comparison of the proposed model prediction (solid lines) with experimental results of [31].

3.3 Torsion of thin wires

The third example concerns the simulation of the torsion tests conducted by Fleck and co-workers [17] on thin wires to obtain experimental evidence of the size effect at the microscale in ductile materials. These tests have been used by many authors [2, 4, 23] to validate the proposed nonlocal models.

Let us consider a circular wire of radius R, diameter $D = 2R$, subject to a torque M (Figure 7). The only nonzero stress and strain components are the tangential stress τ and the shear strain γ, which varies with radius r from the axis x_3 of twist

$$\gamma = \phi r = \gamma^e + \gamma^p \qquad \tau = G\gamma^e \tag{23}$$

ϕ is the twist per unit length of the wire. Torque and tangential stress are related through equilibrium

$$M = 2\pi \int_0^R \tau r^2 \mathrm{d}r \tag{24}$$

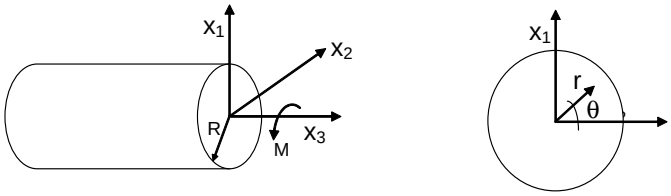

Figure 7: Torsion of thin wires: coordinate systems.

Due to the axisymmetry of the problem, there is no dependence on the angle θ in the response.

The general expressions for the nonlocal yield function (6) and the evolutive equations (3) can be simplified as

$$\bar{f} = G(\bar{\gamma} - \gamma^p) - \chi(\eta), \qquad \dot{\gamma}^p = \dot{\eta} = \dot{\lambda} \tag{25}$$

where $\bar{\gamma}$ is the nonlocal shear strain defined according to (4) and taking into account the axial-symmetry of the problem

$$\bar{\gamma}(r) = \int_0^R W(r-s)\,\gamma(s)\,\mathrm{d}s \tag{26}$$

Non-linear hardening is assumed in the form

$$\chi = \tau_y + k\eta^N = \tau_y + k\,(\gamma^p)^N \tag{27}$$

where τ_y is the yield stress and N is the hardening exponent.

Substituting equation (23)a into equation (4) one has,

$$\bar{\gamma} = \phi\,\frac{2\,\ell\left(r e^{-\frac{r^2}{2\,\ell^2}} - (R+r)e^{-\frac{(R-r)^2}{2\,\ell^2}}\right) + \sqrt{2\,\pi}\,\left(\ell^2 + r^2\right)\,\left(\mathrm{Erf}(\frac{R-r}{\sqrt{2}\,\ell}) + \mathrm{Erf}(\frac{r}{\sqrt{2}\,\ell})\right)}{2\,\ell\left(-e^{\frac{-(R-r)^2}{2\,\ell^2}} + e^{\frac{-r^2}{2\,\ell^2}}\right) + \sqrt{2\,\pi}\,r\,\left(\mathrm{Erf}(\frac{R-r}{\sqrt{2}\,\ell}) + \mathrm{Erf}(\frac{r}{\sqrt{2}\,\ell})\right)} \tag{28}$$

where,

$$\mathrm{Erf}(x) = \frac{2}{\sqrt{\pi}}\int_0^x e^{-t^2}\mathrm{d}t \tag{29}$$

is the function error, i.e., twice the integral of Gaussian distribution with 0 mean and variance of 1/2. Figure 8 presents the $\bar{\gamma}$ profile to different values of R. As the radius R increases, the nonlocal effect decreases and $\bar{\gamma}$ tends to its local value γ.

When $r = R$, $\bar{\gamma}$ achieves its maximum value $\bar{\gamma}_R$, defined by,

$$\bar{\gamma}_R = \phi\,\frac{2\,R\left(-2 + e^{\frac{-R^2}{2\,\ell^2}}\right)\,\ell + \left(R^2 + \ell^2\right)\,\sqrt{2\,\pi}\,\mathrm{Erf}(\frac{R}{\sqrt{2}\,\ell})}{2\left(-1 + e^{\frac{-R^2}{2\,\ell^2}}\right)\,\ell + R\,\sqrt{2\,\pi}\,\mathrm{Erf}(\frac{R}{\sqrt{2}\,\ell})} \tag{30}$$

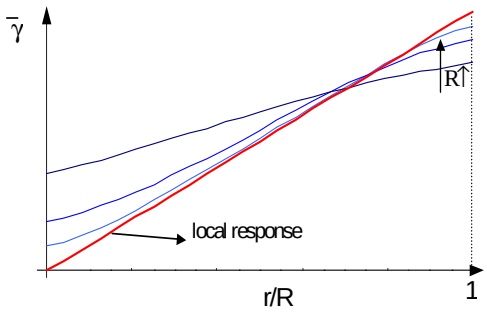

Figure 8: Profile of the nonlocal shear strain for different wire size R

G	k	N	τ_y	ℓ
30 GPa	117 MPa	0.23	113 MPa	0.5 μm

Table 1: Set of material parameters.

For the numerical example, the values in Table 1 where adopted, in order to capture the experimental results obtained in [17] and shown in Figure 9a.

The solution obtained with the proposed model is given by Figure 9b. For varying radius, the model gives a qualitatively correct prediction of the size effect in the plastic response.

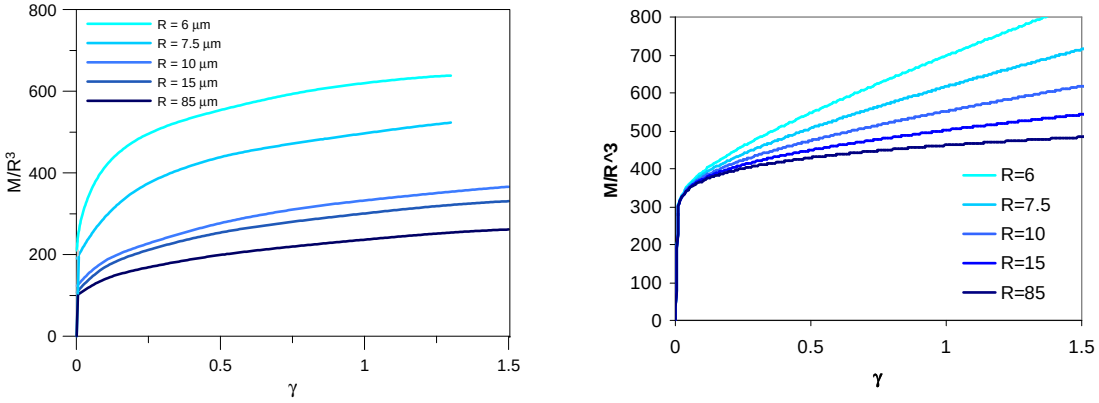

(a) (b)

Figure 9: Normalized torque versus normalized twist at $r = R$ (a) experimental results from [17]; (b) simulation with constant yield stress.

In order to illustrate the decrease of gradient effect when the radius increases, in Figure 10 different length scale parameters are considered for radii $R = 10$ μm and $R = 85$ μm. It can be

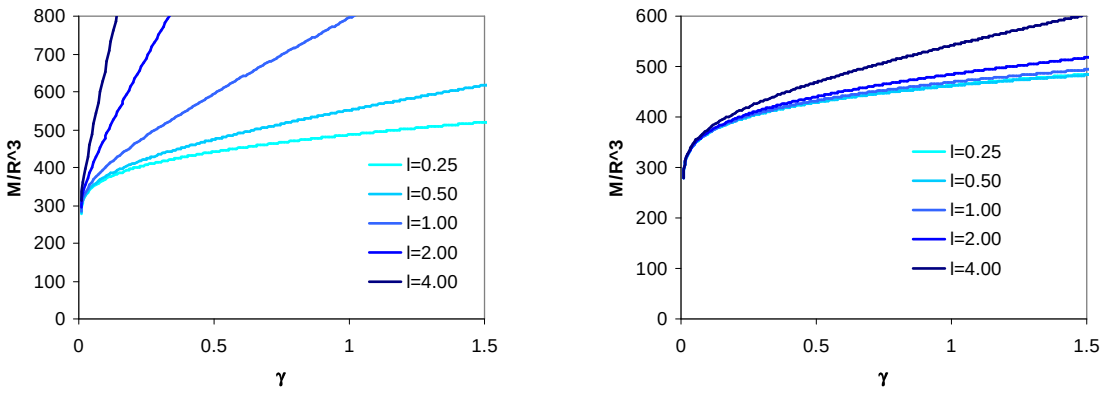

Figure 10: Effect of material length ℓ (a) $R = 10\mu m$; (b) $R = 85\mu m$

seen that the nonlocal effect is more evident for small specimen size.

4 Conclusions

A simple elastoplastic nonlocal model is proposed in order to deal with phenomena which are not well represented by conventional continuum theories, such as localization and size–dependence in micron-sized structures. From the theoretical point of view, the model introduces an internal length and ensures well-posedness of the boundary value problem also in the presence of softening. Numerically, the proposed model presents no difficulties in the implementation, since the nonlocal variable – total strain – is the input, driving quantity in the solution of nonlinear constitutive equations. The nonlocal corrector phase can still be performed locally, at the Gauss point level. The simple one-dimensional examples shown in this paper confirm the potentiality of the proposed model. Application to more realistic problems exhibiting size effects, such as the totally not standardized microtensile tests adopted by the dentistry to evaluate the strength of a resin [12], is currently in progress.

Acknowledgements: The work has been carried out within the context of MIUR-PRIN 2003082105 research project. The second author acknowledges the financial support of FAPESP (Brazil).

References

[1] A. Acharya and J. L. Bassani. Lattice incompatibility and a gradient theory of crystal plasticity. *Scripta Materialia*, 48:167–172, 2000.

[2] E. C. Aifantis. Strain gradient interpretation of size effects. *International Journal of Fracture*, 95:299–314, 1999.

[3] M. Atkinson. Further analysis on the size effect in indentation hardness tests of some metals. *Journal of Materials Research*, 10:2905–2915, 1995.

[4] J. L. Bassani. Incompatibility and a simple gradient theory of plasticity. *Journal of the Mechanics and Physics of Solids*, 49:1983–1996, 2001.

[5] Z.P. Bazant. Size effect on structural length: a review. *Archives in Applied Mechanics*, 69:703–725, 1999.

[6] Z.P. Bazant and T. Belytschko. Wave propagation in a strain softening bar:exact solution. *Journal of Engineering Mechanics*, 111(3):381–389, 1984.

[7] A. Benallal, R. Billardon, and G. Geymonat. Some mathematical aspects of the damage softening problems. In *Cracking and Damage - J. Mazars; Z.P. Bazant (eds.)*, pages 247–258. Elsevier,Amsterdam, 1988.

[8] C. Comi. Computational modelling of gradient-enhanced damage in quasi-brittle materials. *MCFM*, 4(1):17–36, 1999.

[9] C. Comi. A non-local model with tension and compression damage mechanisms. *European Journal of Mechanics, A/Solids*, 20:1–22, 2001.

[10] C. Comi and L. Driemeier. On gradient regularization for numerical analysis in the presence of damage. In *Material Instabilities in Solids - de Borst, R.; van der Giessen, E. (eds), chapter XVI*, pages 425–440, 1998.

[11] C. Comi and L. Driemeier. A nonlocal plasticity model: size effect and localization. In *Proceedings of XXV CILAMCE, Recife Pernambuco, Brasil*, November 2004.

[12] Josete da Cruz Meira, Rafael Yagüe, Roberto Martins, and Larissa Driemeier. On concentration factor in microtensile tests. *Journal of Adhesive Dentistry*, 4:267–273, 2004.

[13] R. de Borst, M. Heeres, and A. Benallal. A gradient enhanced damage model: theory and computation. In *Computational Plasticity: Fundamentals and applications, D.R.J.Owen, E.Onate, E.Hinton (eds.), Complas IV*, pages 975–986. Pineridge-Press, 1995.

[14] R. de Borst and B. Muhlhaus. Continuum models for discontinuous media. In *Fracture processes in concrete, rock and Ceramics , J. G. M. van Mier, J. G. Rots, A. Bakker (eds.)*, pages 601–618, 1991.

[15] J. Fish, W. Chen, and G. Nagai. Nonlocal dispersive model for wave propagation in heterogeneous media. parts i and ii. *International Journal of Numerical Methods in Engineering*, 54:331–363, 2002.

[16] N. A. Fleck and J. W. Hutchinson. Strain gradient plasticity. *Archives in Applied Mechanics*, 33:295–361, 1997.

[17] N. A. Fleck, G. M. Muller, M. F. Ashby, and J.W.Hutchinson. Strain gradient plasticity: theory and experiment. *Acta Metallica Materialia*, 42(2):475–487, 1994.

[18] N.A. Fleck and J.W. Hutchinson. A phenomenological theory for strain gradient effects in plasticity. *Journal of the Mechanics and Physics of Solids*, 41(12):1825–1857, 1993.

[19] H. Gao and Y. Huang. Taylor-based nonlocal theory of plasticity. *International Journal of Solids and Structures*, 38:2615–2637, 2001.

[20] H. Gao, Y. Huang, W. Nix, and J. W. Hutchinson. Mechanism-based strain gradient plasticity - i. theory. *Journal of the Mechanics and Physics of Solids*, 47:1239–1263, 1999.

[21] M.A. Haque and M.T.A. Saif. Strain gradient effect in nanoscale thin films. *Acta Materialia*, 51:3053–3061, 2003.

[22] R. Hill. *The Mathematical theory of Plasticity*. Oxford University Press, 1st edition, 1950.

[23] Y. Huang, H. Gao, W. Nix, and J. W. Hutchinson. Mechanism-based strain gradient plasticity - i. analysis. *Journal of the Mechanics and Physics of Solids*, 48:99–128, 2000.

[24] R. M. McMeeking and J. R. Rice. Finite element formulations for problems of large elasto-plastic deformation. *International Journal of Solids and Structures*, 11:601–616, 1975.

[25] A. Menzel and P. Steinmann. On the continuum formulation of higher gradient plasticity for single and polycrystals. *Journal of the Mechanics and Physics of Solids*, 49:1777–1796, 2000.

[26] C. F. Niordson and J.W. Hutchinson. On lower order strain gradient plasticity theories. *European Journal of Mechanics, A/Solids*, 22:771–778, 2003.

[27] W.D. Nix. Mechanical properties of thin films. *Metall. Trans.*, 20:2217–2245, 1989.

[28] W.D. Nix and H. Gao. Indentation size effects in crystalline materials: a law for strain gradient plasticity. *Journal of the Mechanics and Physics of Solids*, 46(3):411–425, 1998.

[29] G. Pijaudier-Cabot and Z. L. Bazant. Nonlocal damage theory. *Journal of Engineering Mechanics*, 113:1512–1533, 1987.

[30] P. Steinmann and E. Stein. Finite element localization analysis of micropolar strength degrading materials. In *Computer modelling of concrete structures, Mang, H.; Bicanic, N.; de Borst, R. (eds.)*, pages 435–444. North-Holland Publ. Comp., 1994.

[31] J. S. Stolken and A. G. Evans. A microbend test for measuring the plasticity length scale. *Acta Materialia*, 36(14):5109–5115, 1998.

[32] M.F. Ashby W.J. Poole and N.A. Fleck. Microhardeness of annealed and work-hardened copper polycrystals. *Scripta Metall. Mater.*, 34:559–564, 1996.